Mechanism of the Chain Termination of the Allylnickel(II)-Catalyzed Polymerization of 1,3-Butadiene. A Density Functional Investigation for the Cationic $[Ni^{II}(RC_3H_4)(cis\text{-}C_4H_6)L]^+$ Active Catalyst

Sven Tobisch†

Institut für Anorganische Chemie der Martin-Luther-Universität Halle-Wittenberg, Fachbereich Chemie, Kurt-Mothes-Strasse 2, D-06120 Halle, Germany

Received March 24, 2003; Revised Manuscript Received June 19, 2003

ABSTRACT: Alternative mechanisms of chain termination of the allylnickel(II)-catalyzed polymerization of 1,3-dienes have been investigated by employing a gradient-corrected DFT method: namely, (I) the hydrogen transfer mechanism and (II) the hydrogen elimination mechanism. Several conceivable pathways for each of these mechanisms have been scrutinized for the well-characterized *trans*-1,4 regulating cationic allylnickel(II) $[Ni^{II}(\eta^3\text{-}RC_3H_4)(cis\text{-}C_4H_6)L]^+$ active catalyst. The transfer of a hydrogen atom from the C^4-(butenyl) carbon of the growing polymer chain to the coordinated monomer, which starts with the butadiene π-complex, is suggested to be the favorable mechanism of chain termination. This process is found to preferably proceed in a concerted fashion outside of the immediate proximity of the nickel atom. On the other hand, the hydrogen elimination occurring from the monomer insertion product by hydrogen abstraction from the polymer chain (C^4(butenyl) carbon) yielding initially an diene hydride species, is seen to be kinetically disfavored. Accordingly, hydrogen elimination represents a less likely channel for chain termination. The monomer π-complex is the crucial species of the entire polymerization reaction course, as it serves as the precursor for the critical monomer insertion and allylic *anti*−*syn* elementary steps of the chain propagation cycle, as well as for the favorable hydrogen transfer chain termination channel. The present study provides, for the first time, a theoretically well-founded insight into the mechanism of molecular weight regulation for the allylnickel(II)-catalyzed polymerization of 1,3-dienes.

Introduction

A broad variety of transition-metal-based catalysts, with one-component allyl−transition-metal complexes and Ziegler−Natta catalyst systems as principal examples, have been established[1] that actively catalyze the polymerization of 1,3-dienes in a highly chemo-, regio-, and stereoselective fashion.[2] Among the various catalysts, structurally well-defined (η^3-allyl)nickel(II) complexes, in particular, represent catalysts that were studied in the most detailed way by experiment. The following types of allylnickel(II) complexes, that promote almost exclusively the generation of 1,4-polybutadienes, are known: (i) the neutral dimeric allylnickel(II) halides and halogenoacetates $[Ni^{II}(\eta^3\text{-}RC_3H_4)X]$ (X = Cl, Br, I,[3] CF_3CO_2, CCl_3CO_2 [4]), which in the case of the halides afford a polybutadiene consisting predominantly of a *cis*-1,4 (X = Cl), and of a *trans*-1,4 structure (X = I), or of a statistical equibinary 1,4-polybutadiene (X = Br); (ii) the *trans*-1,4 regulating cationic butenyl(monoligand)-(butadiene)nickel(II) $[Ni^{II}(\eta^3\text{-}RC_3H_4)(C_4H_6)L]^+$ active catalyst complexes (L = PR_3, $P(OR)_3$);[5] and (iii) the *cis*-1,4 regulating cationic polybutadienyl(butadiene)nickel-(II) $[Ni^{II}(\eta^3,\eta^2\text{-}RC_7H_{10})(C_4H_6)]^+$,[6] active catalyst. In a series of investigations, we have previously explored computationally the entire chain propagation cycles, consisting of competing paths for monomer insertion and of allylic *anti*−*syn* isomerization, for all these different types of catalysts.[7] This enabled us to derive a theoretically well-founded, comprehensive view of the cis−trans regulation for the allylnickel(II)-catalyzed 1,4-polymerization of butadiene.[8]

Besides activity and selectivity, the molecular weight and molecular weight distribution of the generated polydiene are among the most important properties that characterize a particular catalyst. The *trans*-1,4 regulating crotylnickel(II) iodide[9] and the cationic polybutadienyl(butadiene)nickel(II) *cis*-1,4 active catalyst[10] were the subject of a detailed experimental investigation of the molecular weight regulation of the allylnickel(II)-catalyzed polymerization of 1,3-butadiene, affording polybutadienes of $M_n \sim 5300$ g mol^{-1} [11a] and $M_n \sim 32\,000$ g mol^{-1},[11b,c] respectively, under standard conditions. For both types of catalysts, it was shown that the molecular weight is nearly unaffected under variation of noncoordinating solvents and temperature. The latter would imply a similar temperature dependence of the dominant chain propagation and chain termination processes.

It has been unequivocally established by experiment that the chain transfer process leads to the formation of a 1,3-diene terminated polydiene chain.[10,12] Accordingly, an operative chain termination mechanism is likely to involve the abstraction of a hydrogen atom from the C^4 carbon of the terminal reactive butenyl group of the growing polymer chain. Among several conceivable mechanisms, the following are the two most probable for chain termination.

On one hand, chain termination can proceed without being assisted by the coordinated monomer (hydrogen elimination mechanism; cf. Scheme 1). It is thus likely to commence from the kinetic insertion product, occurring in a multistep fashion, with the first step being the hydrogen elimination from the growing polydienyl chain (C^4(butenyl) carbon) to the transition metal. This gives rise to a hydride complex carrying the diene-terminated polymer chain. In subsequent steps incoming monomer displaces the diene-terminated chain, either in a dissociative or associative fashion depending on the cata-

† E-mail: tobisch@chemie.uni-halle.de.

10.1021/ma034369v CCC: $25.00
Published on Web 07/19/2003

Scheme 1. Hydrogen Elimination Mechanism[a]

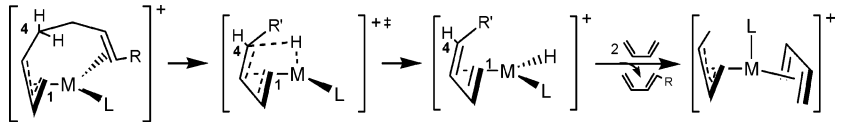

[a] Exemplified for the *anti*-η^3 form of the of the growing polydienyl chain.

Scheme 2. Hydrogen Transfer Mechanism[a]

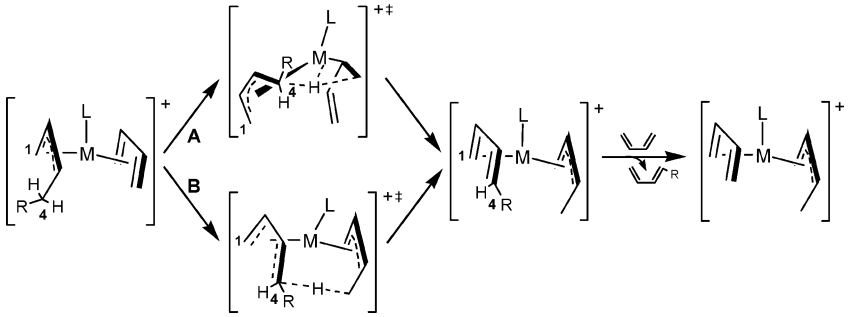

[a] Exemplified for the *anti*-η^3 form of the of the growing polydienyl chain.

lyst structure, followed by insertion of a second monomer into the hydrido−transition-metal bond to yield the η^3-butenyl monomer π-complex, which can initiate a new chain.

On the other hand, the coordinated monomer can act to actively assist the chain transfer (hydrogen transfer mechanism, cf. Scheme 2). This mechanism is characterized by the hydrogen shift from the growing chain (C^4(butenyl) carbon) to the monomer occurring from the monomer π-complex as the precursor, and giving rise to a η^3-butenyl−transition-metal complex with the diene-terminated chain. After the new monomer displaces the terminated polydiene chain in an associative or dissociative fashion, the catalytically active monomer π-complex is regenerated, which starts the regrowth of a new chain via monomer insertion into the η^3-butenyl−transition-metal bond. Two paths are imaginable for the hydrogen transfer mechanism. First, the hydrogen transfer can occur in close vicinity to the transition-metal (path A in Scheme 2, denoted as inner-sphere hydrogen transfer path), which may take place either in a concerted fashion or through a formal multistep process, involving the formation of a transition-metal hydride intermediate. Alternatively, the hydrogen atom can shift outside of the immediate proximity of the transition-metal (path B in Scheme 2, denoted as outer-sphere hydrogen transfer path) through a concerted process.

Given the importance of the understanding of the chain termination for elucidating the mechanism of molecular weight regulation, it is surprising that no reliable computational investigation addressing the mechanism of chain termination for the transition-metal-catalyzed 1,3-diene polymerization has been reported so far. The present computational study examines in detail several imaginable reaction paths for the hydrogen elimination and hydrogen transfer mechanisms, aimed at identifying the most feasible mechanism of chain termination for a prototypical allylnickel(II) catalyst. The investigation is conducted for the experimentally well-characterized highly *trans*-1,4 selective cationic $[Ni^{II}(\eta^3\text{-}RC_3H_4)(C_4H_6)L]^+$ active catalyst.[5] In this first theoretical mechanistic exploration of chain termination, the primary goal is to present a basic view of intimate details of the process, in terms of located key structures and the energetic profile for different reaction routes. In this approach, factors that are related to a counterion, a solvent, or steric congestion caused by a bulky, space-demanding ligand are neglected, although they may influence chain propagation and chain termination to a different magnitude. Finally, an insight into the mechanism of molecular weight regulation in the allylnickel(II)-catalyzed polymerization of 1,3-dienes will be provided, based on the comparison of the favorable reaction routes for chain propagation and chain termination.

First, hydrogen elimination and hydrogen transfer will be discussed in the context of the chain propagation cycle (cf. Scheme 3 parts a and b), that has been established both by experimental[1f,5d,13] and theoretical[7b,e,8] evidence for the catalyst under investigation. The peculiar mechanistic aspects of 1,3-diene polymerization will not be repeated here in detail since they can be found elsewhere.[8,13,14]

Catalytic Reaction Course Comprising Chain Propagation and Chain Termination

The butadiene π-complex $[Ni^{II}(\eta^3\text{-}RC_3H_4)(C_4H_6)L]^+$ is the catalytically active species for chain propagation. Starting from the $[Ni^{II}(\eta^3\text{-}C_3H_5)L_2]^+$ precatalyst **1**, the monomer π-complex is formed by substitution of the ligand L by butadiene. The position of the substitution equilibrium is far on the side of the precatalyst **1** (cf. Scheme 3a). The π-complex exists in several forms and isomers, all of which are in equilibrium. Thermodynamically favorable is the formal 18e$^-$ η^3-butenyl/*cis*-η^4-butadiene form **2**, with the alternatively occurring formal 16e$^-$ η^3-butenyl/*cis*-η^2-butadiene form **2′** is higher in energy. There are two isomeric *syn*-η^3 and *anti*-η^3 forms[15d] of the butenyl−Ni^{II} coordination (for example, **2s**, **2a** for the *cis*-η^4-butadiene π-complex **2**,[15d] cf. Scheme 3a,b), with the *syn* form being more stable. Furthermore, for **2** (and **2′** as well) there are several isomers, that are distinguished by the mutual arrangement of the butenyl and butadiene moieties. Concerning **2**, the thermodynamically favorable isomer arises from a supine (exo)[16] orientation of both the butenyl and butadiene moieties (**2a**/**2s**-SS), while prone (endo)[16] butadiene isomers (f.i. **2a**/**2s**-PP) are involved during monomer insertion.

Chain propagation preferably takes place via *cis*-butadiene insertion into the η^3-butenyl−Ni^{II} bond (**2** →

Scheme 3. (a) Generation of the [Ni^{II}(η^3-RC$_3$H$_4$)(cis-η^4-C$_4$H$_6$)L]$^+$ Active Catalyst 2 from the [Ni^{II}(η^3-RC$_3$H$_4$)L$_2$]$^+$ Precatalyst 1, Together with Allylic *Anti*−*Syn* Isomerization[15a] and (b) Catalytic Reaction Course of the *trans*-1,4 Generating Channel of the Allylnickel(II)-Catalyzed 1,4-Polymerization of 1,3-Butadiene Promoted by the Cationic [Ni^{II}(η^3-RC$_3$H$_4$)(*cis*-η^4-C$_4$H$_6$)L]$^+$ Active Catalyst, Consisting of Monomer Insertion (along k_{1t}, (k_{1c})), Allylic *Anti*−*Syn* Isomerization (along $k_{a/s}$), and Chain Termination via Hydrogen Transfer (along k_{ht}) and via Hydrogen Elimination (along k_{he})[15]

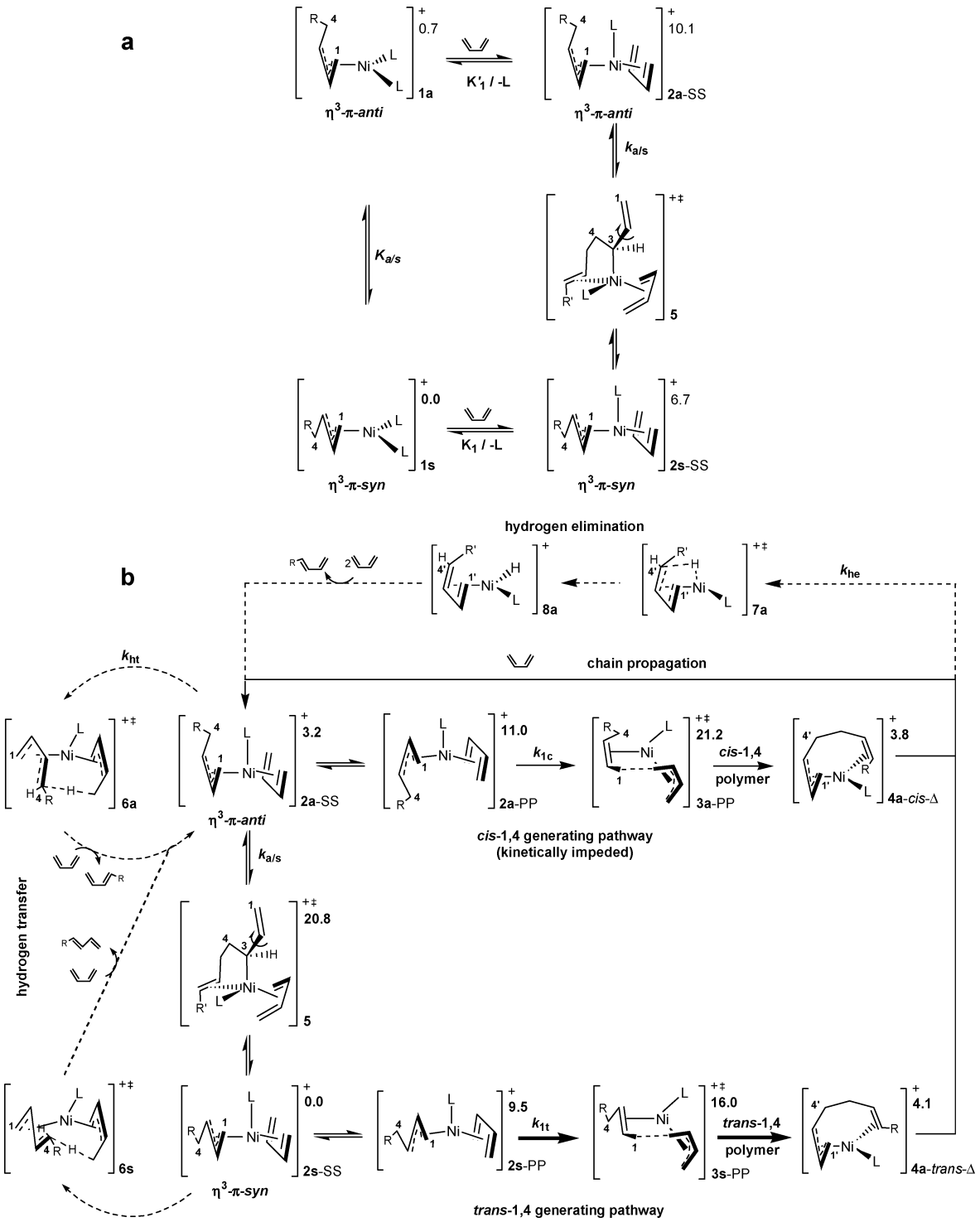

3 → **4a**, Scheme 3b) according to the π-allyl insertion mechanism proposed by Taube et al.[1f,13,17] The reacting moieties adopt a quasi-planar four-membered cis arrangement in the corresponding transition state **3**, thus restricting the butadiene to a prone (endo)[16] orientation (cf. Scheme 3b). However, the σ-allyl insertion mechanism, suggested as an alternative,[18] has been demonstrated to not be operative in both the allylnickel(II)-[7,8] as well as in the allyltitanium(III)-catalyzed[19] 1,3-diene polymerization. *trans*-1,4 polymer units are formed by *cis*-butadiene insertion into the *syn*-η^3-butenyl−Ni^{II} bond along the k_{1t} insertion pathway (**2s**-SS → **2s**-PP → **3s**-PP → **4a**-*trans*-Δ), which is kinetically preferred relative to the competing k_{1c} pathway (**2a**-SS → **2a**-PP → **3a**-PP → **4a**-*cis*-Δ) for generation of *cis*-1,4 polymer units. This always affords the *anti*-η^3-butenyl terminal group of the growing polybutadienyl chain in the kinetic insertion product **4a**. The insertion of butadiene from

its s-trans configuration, however, is suppressed on kinetic considerations.[20] The isomerization of *anti* and *syn* isomers of the η^3-butenyl−Ni^{II} bond favorably proceeds in accordance with experimental indications,[21] commencing from **2a** by means of a η^3-$\pi \rightarrow \eta^1$-σ-C^3-butenyl group conversion, followed by internal rotation of the vinyl group via transition state **5** and rearrangement into the *syn*-η^3 form **2s**.[22] Allylic isomerization along $k_{a/s}$ is an indispensable step in the polymerization course for the generation of *trans*-1,4 polymer units, and has been unambiguously established by NMR experiments to be rate-controlling in the chain propagation cycle.[5d]

The high 1,4-*trans* selectivity of the $[Ni^{II}(\eta^3\text{-}RC_3H_4)(\textit{cis}\text{-}\eta^4\text{-}C_4H_6)L]^+$ active catalyst complex is decisively determined by two factors. First, the thermodynamically favorable *syn*-η^3-butenyl form displays a higher proclivity to undergo *cis*-butadiene insertion when compared to the *anti* form ($k_{1t} > k_{1c}$). Second, allylic *anti*−*syn* isomerization, although it is rate-determining, is facile enough to make the *trans*-1,4 pathway k_{1t} accessible; thus $k_{1t} > k_{a/s} > k_{1c}$ is valid. Consequently, the less reactive *anti* form should be enriched in the reaction solution under polymerization conditions, while the *syn* form practically does not exist in a detectable amount due to its higher reactivity. These aspects are consistent with experimental observation.[5d]

Chain termination via the hydrogen transfer mechanism is likely to commence from the same catalyst complex as chain propagation does. Accordingly, the *cis*-η^4-butadiene π-complex **2** represents the critical species in the catalytic polymerization course that acts as the precursor for the monomer insertion (preferably via k_{1t}), allylic *anti*−*syn* isomerization ($k_{a/s}$) and hydrogen transfer (k_{ht}) elementary steps. Hydrogen transfer occurring through transition state **6**[15e] that starts from **2a** and **2s** always leads to the regeneration of the *anti*-η^3-butenyl group as the initial point for chain regrowth, together with a diene-terminated polymer chain of cis and trans configurations, respectively. The diene-terminated chain is subsequently displaced by incoming butadiene, which regenerates **2a**. The *syn* form **2s**, however, is accessible only via the rate-determining *anti*−*syn* isomerization (**2a** → **5** → **2s**), and **2s** is likely to immediately undergo monomer insertion along the k_{1t} pathway. Consequently, the hydrogen transfer via **6s** is less likely to occur due to the very low stationary concentration of **2s** when compared with **2a** (vide supra) and this process is most probable to proceed through transition state **6a**.

Instead, the hydrogen elimination process along k_{he} starts from the insertion product **4a**-*trans*-Δ and affords the diene hydride complex **8a** via transition state **7a**.[15f] Compound **8a** reacts further to give fast **2a** through consecutive displacement of the diene-terminated chain by new monomer and insertion of a second butadiene into the hydrido−nickel bond. Thus, different precursor species are involved in monomer insertion (preferably via k_{1t}) and allylic isomerization ($k_{a/s}$) on one hand, and hydrogen elimination (k_{ht}) on the other.

Similar to both chain termination mechanism along k_{he} and k_{ht} is the fact that *anti*-butenyl forms, namely **4a**-*trans*-Δ and **2a**, are likely to represent the respective precursor species.

Computational Model and Method

Model. The hydrogen elimination and hydrogen transfer mechanisms were examined by adopting the cationic $[Ni^{II}(\eta^3\text{-}RC_3H_4)(\textit{cis}\text{-}C_4H_6)P(OMe)_3]^+$ complex as a computationally practicable model of the real *trans*-1,4-regulating $[Ni^{II}(\eta^3\text{-}RC_3H_4)(C_4H_6)L]^+$ catalyst, which is derived from the well-characterized $[Ni^{II}(\eta^3\text{-}C_3H_5)(P(OPh)_3)_2]PF_6$ precatalyst.[5] In the investigation of the hydrogen elimination (k_{he}), the growing polybutadienyl chain consisted of two C_4-polymer units; i.e., η^3,η^2-C_8H_{13} in precursor **4a**-*trans*-Δ. Preliminary investigations indicated the pentenyl group (η^3-C_5H_9) to be suitable for mimicking the polybutadienyl chain in the butadiene π-complex **2**, which ensures a realistic description of the hydrogen transfer process (k_{ht}).

The effect of the solvent and the counterion was neglected in the present study, which is aimed at the elucidation of principal mechanistic aspects of the chain termination process. The mechanistic conclusions drawn in the present study, therefore, are valid for polymerization occurring in noncoordinating solvents with weakly coordinating counterions involved. Furthermore, the ejection process of the diene-terminated polymer chain is not considered in full detail by the present study.

Method. All reported DFT calculations were performed by using the TURBOMOLE program package developed by Häser and Ahlrichs.[23] The local exchange-correlation potential by Slater[24a,b] and Vosko et al.[24c] was augmented with gradient-corrected functionals for electron exchange according to Becke[24d] and correlation according to Perdew[24e] in a self-consistent fashion. This gradient-corrected density functional is usually termed BP86 in the literature. In recent benchmark computational studies it was shown that the BP86 functional gives results in excellent agreement with the best wave function-based method available today, for the class of reactions investigated here.[25]

For all atoms a standard all-electron basis set of triple-ζ quality for the valence electrons augmented with polarization functions was employed for the geometry optimization and the saddle-point search. The Wachters 14s/9p/5d set[26a] supplemented by two diffuse p[26a] and one diffuse d function[26b] contracted to (62111111/5111111/3111) was used for nickel, and standard TZVP basis sets[26c] were employed for phosphorus (a 13s/9p/1d set contracted to (73111/6111/1)), for carbon, oxygen (a 10s/6p/1d set contracted to (7111/411/1)), and for hydrogen (a 5s/1p set contracted to (311/1)). The frequency calculations were done using standard DZVP basis sets,[26c] which consist of a 15s/9p/5d set contracted to (63321/531/41) for nickel, a 12s/8p/1d set contracted to (6321/521/1) for phosphorus, a 9s/5p/1d set contracted to (621/41/1) for carbon and oxygen, and a 5s set contracted to (41) for hydrogen, for DZVP-optimized structures, which differ in marginal extent from the triple-ζ-optimized ones. The corresponding auxiliary basis sets were used for fitting the charge density.[26c,d]

The geometry optimization and the saddle-point search were carried out at the BP86 level of approximation by utilizing analytical/numerical gradients/Hessians according to standard algorithms. No symmetry constraints were imposed in any case. The stationary points were identified exactly by the curvature of the potential-energy surface at these points corresponding to the eigenvalues of the Hessian. All reported transition states possess exactly one negative Hessian eigenvalue, while all other stationary points exhibit exclusively positive eigenvalues. The several isomers that are possible for each species **6**−**8** in Scheme 3b were carefully explored. Only the most stable isomers of each of the key species of the several investigated paths for chain termination were reported, for which the reaction and activation free energies (ΔG, $\Delta G^{\ddagger}$ at 298 K and 1 atm) were calculated. The educt and product that corresponded directly to the located transition-state structure were verified by following the reaction pathway going downhill to both sides from slightly relaxed transition-state structures. The electronic structure of key stationary points was analyzed with the natural bond orbital (NBO) population scheme.[27]

Results and Discussion

We shall start our investigation by scrutinizing several reaction paths for each of the hydrogen elimina-

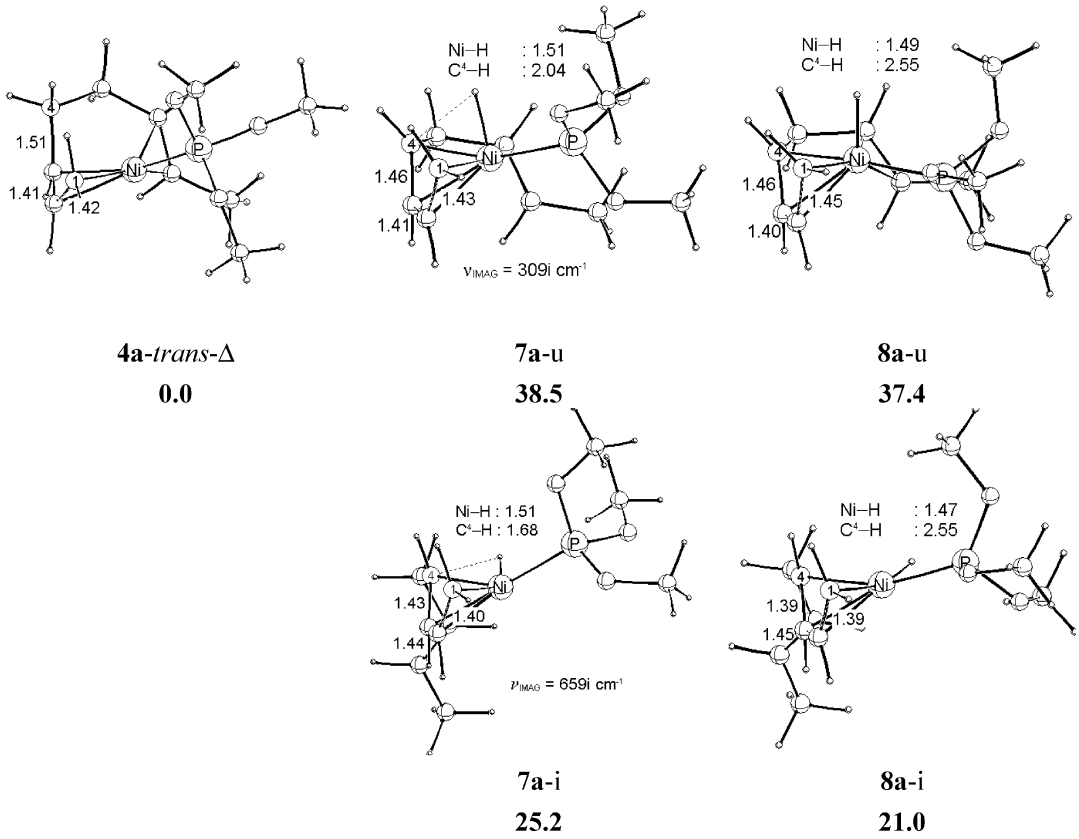

Figure 1. Upright (top) and inplane (below) pathways of the hydrogen elimination mechanism. Selected geometric parameters [Å] of the optimized structures of key species are given, together with Gibbs free energies (kcal mol^{-1}) relative to the [Ni^{II}(η^3,η^2-C_8H_{13})L]$^+$ (L = P(OMe)$_3$) precursor **4a**-*trans*-Δ.

tion and hydrogen transfer mechanisms, that leads us to suggest the operative mechanism of chain termination. On the basis of the insight gained from the present and previous[7b,d,8] computational studies on the critical chain termination and chain propagation processes of the polymerization reaction course, the mechanistic implications for the molecular weight regulation will be elucidated.

A. The Hydrogen Elimination Mechanism. This mechanism, as shown in Scheme 3b, proceeds from the kinetic insertion product **4a**-*trans*-Δ of the k_{1t} insertion path. Commencing from the formal 16e$^-$ square-planar precursor **4a**-*trans*-Δ two pathways for hydrogen elimination from the C^4(butenyl) carbon of the polymer chain to the nickel have been located, distinguished by the position that the hydrogen atom occupies in the diene hydride complex **8a**. These pathways are characterized by the hydrogen shift occurring perpendicular or coplanar to the square-planar coordination plane in **4a**-*trans*-Δ to afford a five-coordinate square-pyramidal **8a**-u, with the hydrogen atom situated in apical position, or a 4-coordinate square-planar **8a**-i, respectively. Along the first pathway (**4a**-*trans*-Δ → **7a**-u → **8a**-u, that is denoted as upright), the first double bond of the growing polymer chain remains coordinated to the nickel atom. In contrast, the second pathway (**4a**-*trans*-Δ → **7a**-i → **8a**-i, that is denoted as inplane) is accompanied by a displacement of the coordinated polymer chain's double bond by the emerging hydrido−nickel bond. A perusal of the reaction path indicates that this displacement is a smooth process, not involving a significant barrier. Although the respective transition state has not been located, it is anticipated to occur at a significantly lower energy compared to the transition state for the hydrogen elimination process. The key species involved along the upright and inplane pathways are displayed in Figure 1 along with the relative energies.

The transition state for hydrogen elimination, **7a**, exhibits a hydrido−nickel bond that seems to be already almost fully established, and a substantially elongated C^4(butenyl)−H bond with the terminated chain coordinated in bidentate mode; thus **7a** appears productlike. Interestingly, the generated terminal group of the polymer chain displays a different characteristic for the two pathways; it can be characterized to be mainly η^4-enediyl (**8a**-u) and η^4-diene (**8a**-i) in its nature for the upright and inplane pathways. This is also reflected in both the thermodynamic stability of **8a** as well as in the kinetic barrier required for the **4a**-*trans*-Δ → **8a** elimination process. The square-pyramidal **8a**-u, with the hydrogen in the apical position, is predicted to be thermodynamically disfavored by 16.4 kcal mol^{-1} (ΔG) relative to the square-planar product species **8a**-i of the inplane pathway (cf. Figure 1). The elimination barrier follows the same trend. The upright pathway is clearly seen to be kinetically unfeasible ($\Delta G^{\ddagger}$ = 38.5 kcal mol^{-1}, **4a**-*trans*-Δ → **7a**-u) and also to afford the thermodynamically unfavorable **8a**-u species, which is separated from **7a**-u by a barrier of only 1.1 kcal mol^{-1} ($\Delta G^{\ddagger}$). As known from simple molecular orbital considerations, a strong σ-donor, like the formally regarded hydride ion, preferably occupies a basal position in a square-pyramidal five-coordinate d^8-complex.[28] Thus, electronic reasons are decisive for the preference of the inplane pathway, as reflected from both kinetic and thermodynamic aspects.

Overall, for hydrogen elimination to occur along the most feasible inplane pathway **4a**-*trans*-Δ → **8a**-i, an

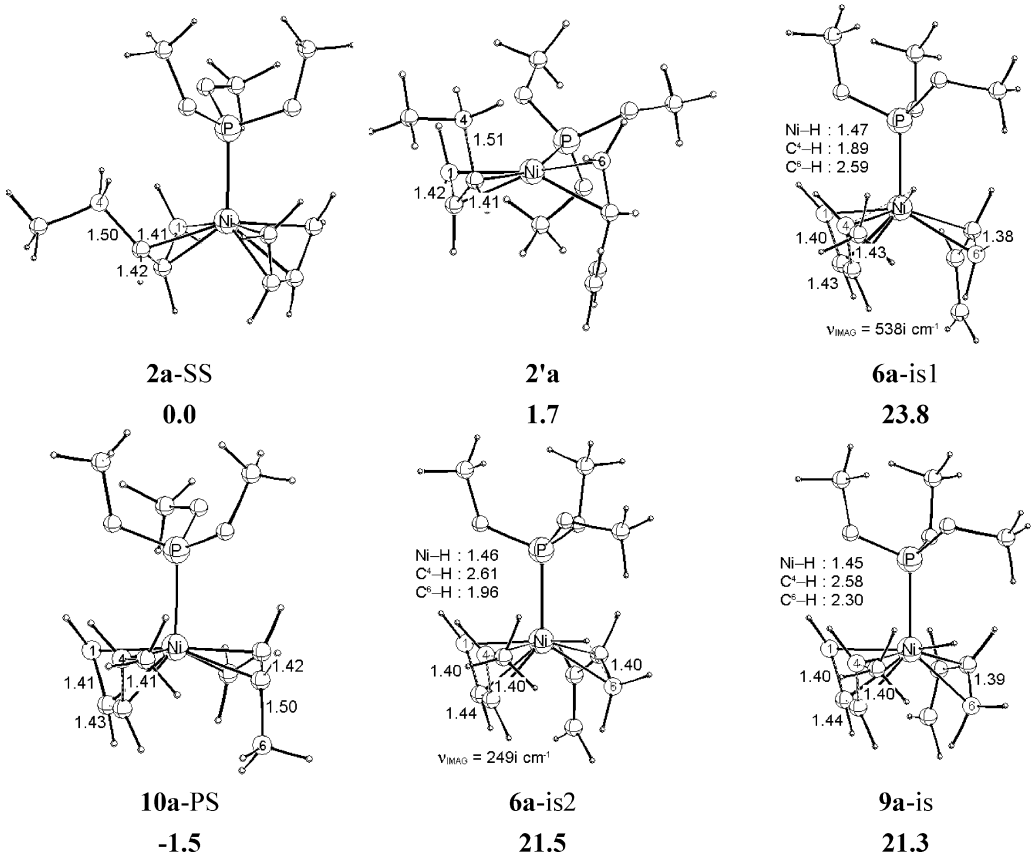

Figure 2. Stepwise inner-sphere pathway of the hydrogen transfer mechanism. Selected geometric parameters [Å] of the optimized structures of key species are given, together with Gibbs free energies (kcal mol^{-1}) relative to the most stable [Ni^{II}(*anti*-η^3-C_5H_9)(*cis*-η^4-C_4H_6)L]$^+$ (L = P(OMe)$_3$) *anti* form of **2**, i.e., **2a**-SS.

activation barrier of 25.2 kcal mol^{-1} ($\Delta G^{\ddagger}$, **4a**-*trans*-Δ → **7a**-i) has to be overcome to yield **8a**-i in a process that is endergonic by 21.0 kcal mol^{-1} (cf. Figure 1). To complete the termination event, the diene-terminated chain must be ejected from the active catalyst site. Commencing from the four-coordinate **8a**-i, this is most likely to proceed via associative displacement with new butadiene, followed by the insertion of a further butadiene into the hydrido−nickel bond, giving rise to **2a**. The overall **8a**-i + 2*cis*-C_4H_6 → **2a**-SS + *cis*-C_8H_{12} process is predicted to be driven by a strong thermodynamic force ($\Delta G = -40.0$ kcal mol^{-1}). The two individual associative displacement and insertion steps have not been examined in detail in the present study. There are, however, clear indications from experiment that these processes are likely to be facile.[29,30] For allylnickel(II) complexes, it can be reasonably supposed, that the first **4a**-*trans*-Δ → **8a**-i step requires the highest barrier overall among all steps involved along k_{he}. In any case, the hydrogen elimination mechanism is accompanied by an activation energy of at least 25.2 kcal mol^{-1} ($\Delta G^{\ddagger}$, **4a**-*trans*-Δ → **7a**-i).

B. The Hydrogen Transfer Mechanism. The *anti*-η^3-butenyl form of the butadiene π-complex is the precursor for the hydrogen transfer from the polybutadienyl chain (C^4(butenyl) carbon) to the coordinated *cis*-butadiene (cf. Scheme 3b) that can be envisioned to be taking place through an inner-sphere or outer-sphere path (as detailed in Scheme 2). In the following section, these two paths will be explored, beginning with the first.

B.1. Inner-Sphere Hydrogen Transfer Path. The inner-sphere path for hydrogen transfer goes along with a formal increase of the coordination number on nickel either when approaching the respective transition state (synchronous process) or by formation of a hydride intermediate (stepwise process). Several pathways have been probed, but in none of the cases could a six-coordinate species be located that would participate in any of them. Accordingly, **2′a** (cf. Figure 2) acts as the direct precursor for the hydrogen transfer process to proceed along the inner-sphere path. Species **2′a** is likely to be populated in sufficient amounts, as it is predicted to be only 1.7 kcal mol^{-1} higher in free energy relative to the most stable *anti* form of **2**, i.e., **2a**-SS.

The careful examination of several possible pathways revealed the following two as the most likely ones. Along a first pathway, the hydrogen transfer takes place in a multistep fashion (cf. Figure 2). Starting from **2′a** with the polybutadienyl chain in supine (exo)[16] orientation, initially a square pyramidal transition state **6a**-is1 is encountered, which constitutes the hydrogen abstraction in the presence of a coordinated monomer. The abstraction is almost accomplished in **6a**-is1 as indicated by a nearly complete formation of both the hydrido−nickel bond and the η^4-diene-terminated chain; thus **6a**-is1 formally exhibits a great similarity to transition state **7a**-i for hydrogen elimination. After overcoming a free-energy barrier of 23.8 kcal mol^{-1} (**2a**-SS → **6a**-is1), **6a**-is1 decays into a stable hydride intermediate **9a**-is, which was confirmed to be a minimum, lying 2.5 kcal mol^{-1} (ΔG) below **6a**-is1. Going further along the reaction path a second transition state **6a**-is2 occurs for hydrogen shift to the coordinated monomer. **6a**-is2 is separated from **9a**-is by a free-energy barrier of only 0.2 kcal mol^{-1}, thus indicating that the hydride species

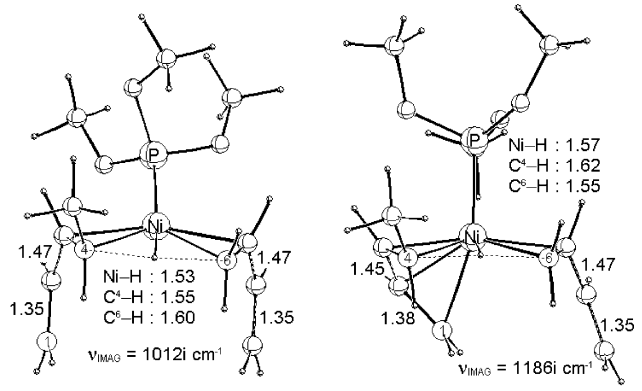

Figure 3. Different configurations of transition state **6a**-ic for the concerted inner-sphere pathway of the hydrogen transfer mechanism. Conventions are as in Figure 2.

9a-is is a highly reactive intermediate occurring in a negligible stationary concentration. The newly formed *anti*-butenyl group rearranges readily into the thermodynamically favorable η^3-π mode, giving rise to the terminated chain product **10a**-PS, which is of a similar constitution of **2a**. Incoming butadiene displaces the terminated chain (most likely in an associative fashion) in a thermoneutral process ($\Delta G = 0.2$ kcal mol^{-1} for **10a**-PS → **2a**-SS) leading to regeneration of **2a**. For the hydrogen transfer process to proceed in a stepwise fashion with an intervening, highly reactive hydride intermediate, a highest barrier of 23.8 kcal mol^{-1} overall ($\Delta G^{\ddagger}$, **2a**-SS → **6a**-is1) for the first hydrogen abstraction step, is required.

In a second instance, the hydrogen transfer takes place in a concerted fashion without a stable hydride intermediate involved. Starting from a precursor **2′a** with the polymer chain in prone (endo)[16] orientation, the η^3-butenyl terminal chain group undergoes transformation into a diene unit along the reaction path, which is almost completed in the transition state **6a**-ic for hydrogen transfer (cf. Figure 3). The pseudo-mirror square-planar **6a**-ic formally constitutes the synchronous hydrogen shift between two coplanar η^2-diene moieties taking place in close proximity to the nickel center (Ni−H distance of 1.53 Å), where the transferring hydrogen atom is at a roughly equal distance from the chain's C^4(butenyl) and the coordinated C^6 of the receiving *cis*-butadiene moiety. Thus, **6a**-ic occurs nearly halfway between educt, **2′a**, and product, **10a**. The question of whether **6a**-ic prefers to adopt a square-planar configuration or not has been explicitly investigated.[31] To this end, several isomers of an alternative trigonal bipyramidal transition state, **6a**-ic′, have been located, where either of the two diene units is coordinated in a bidentate fashion. The energetically favorable one, which is displayed in Figure 3, is seen to be 3.2 kcal mol^{-1} higher in free-energy relative to the square-planar **6a**-ic. An activation barrier of 20.9 kcal mol^{-1} ($\Delta G^{\ddagger}$, **2a**-SS → **6a**-ic) is predicted for the concerted hydrogen transfer through **6a**-ic. The change in the coordination mode of the butenyl group and butadiene moieties along this pathway is likely to proceed readily, as revealed by following the reaction pathway starting from **6a**-ic going downhill both sides.

From the comparison of the energy profile for the two investigated pathways, it becomes clear that the hydrogen transfer process, when occurring in close vicinity to the nickel center is most likely to take place in a concerted fashion via a square-planar, nearly symmetric transition state **6a**-ic, which occurs halfway between educt and product. This pathway has a free-energy barrier of 20.9 kcal mol^{-1} ($\Delta G^{\ddagger}$, **2a**-SS → **6a**-ic), while the alternative stepwise pathway with an intermediately formed stable hydride species **8a**-is is less probable due to the connected kinetic barrier that is 2.9 kcal mol^{-1} higher ($\Delta\Delta G^{\ddagger}$).

Table 1. Charges on Individual Groups at Key Stationary Points of the Concerted Inner-Sphere and Outer-Sphere Pathways of the Hydrogen Transfer Mechanism[a]

species	$\Sigma(C_5H_8)$[b]	H[c]	$\Sigma(C_4H_6)$[d]	Σ(NiL)
2a-SS	−0.222	0.241	−0.047	1.029
6a-ic	−0.021	0.150	−0.046	0.918
6a-oc	−0.106	0.237	−0.143	1.012

[a] On the basis of natural population analysis.[27] [b] Pentenyl moiety without the transferring hydrogen. [c] Transferred hydrogen atom. [d] *cis*-Butadiene moiety.

B.2. Outer-Sphere Hydrogen Transfer Path. The outer-sphere path is distinguished by the following aspect from the inner-sphere path discussed so far. The transferring hydrogen atom does not require an empty coordination site on the nickel atom and accordingly a concerted pathway can be envisioned. The skeletal rearrangements occurring along the outer-sphere path are visible from the located key species, shown in Figure 4 together with the corresponding relative energies. At the initial stage of the process starting from **2a**-SS, the butenyl group and butadiene moieties readily move outside of the immediate proximity of the nickel atom upon changing their coordination mode. The hydrogen transfer proceeds through transition state **6a**-oc, which exhibits characteristics different from those of **6a**-ic. The slightly unsymmetrical trigonal planar **6a**-oc constitutes a transition state for the synchronous transfer of the hydrogen atom between the noncoordinated C^4(butenyl) and C^6 carbons of two reacting allylic moieties (cf. Figure 4). Similar to the inner-sphere path, **6a**-oc occurs nearly halfway between educt, **2a**-SS, and product, **10a**-SS, at roughly equal distances for the breaking and emerging C−H bonds of ∼1.4 Å. Passage through **6a**-oc requires an activation barrier of 18.6 kcal mol^{-1} ($\Delta G^{\ddagger}$, **2a**-SS → **6a**-oc) and yields **10a**-SS as the kinetic product in a slightly exothermic process ($\Delta G = -4.1$ kcal mol^{-1}). The subsequent chain displacement process to complete the termination event has already been discussed in section B.1.

The charges on individual groups for key species of the favorable concerted pathways for inner-sphere and outer-sphere hydrogen transfer collected in Table 1 provide a clear insight into the different nature of the two paths. Along the outer-sphere path through **6a**-oc, the transfer formally takes place between two allylic moieties, with the shifting hydrogen being protonic. In contrast, the inner-sphere path can formally be regarded as a hydride transfer between two butadiene moieties. Which of the two principal paths is more feasible depends essentially on the electronic properties of the [NiL] fragment. It seems likely that the decrease of the electrophilicity of the nickel center due to strong donor phosphines and/or by an enhanced catalyst−counterion interaction could act to impede the inner-sphere transfer path.

So far, several reaction paths for each of the hydrogen elimination and hydrogen transfer mechanisms have

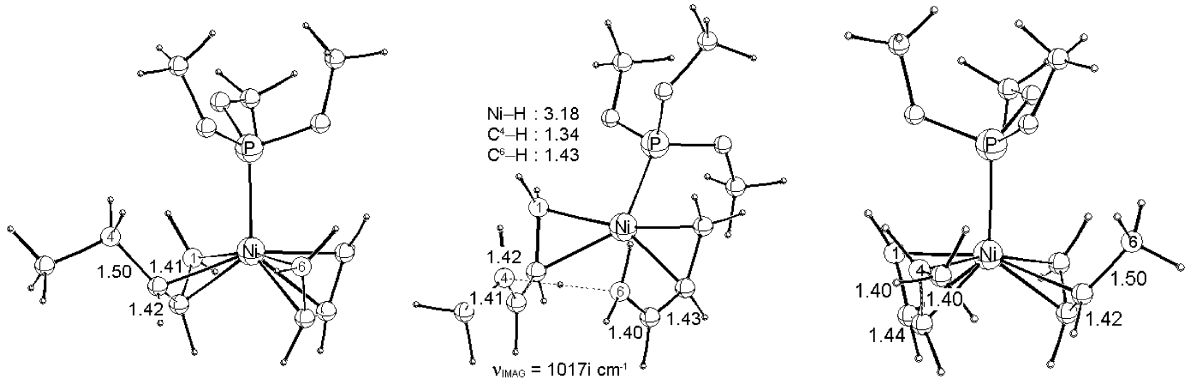

Figure 4. Concerted outer-sphere pathway of the hydrogen transfer mechanism. Conventions are as in Figure 2.

Scheme 4. Condensed Free-Energy Profile of the Catalytic Reaction Course of 1,4-Polymerization of 1,3-Butadiene with the Cationic $[Ni^{II}(\eta^3\text{-}RC_3H_4)(cis\text{-}\eta^4\text{-}C_4H_6)L]^+$ ($R = C_5H_9$, $L = P(OMe)_3$) Active Catalyst, Consisting of *cis*-Butadiene Insertion into the η^3-Butenyl−Ni^{II} Bond, of Allylic *Anti*−*Syn* Isomerization, and of Chain Termination via Hydrogen Transfer[15c,33,34]

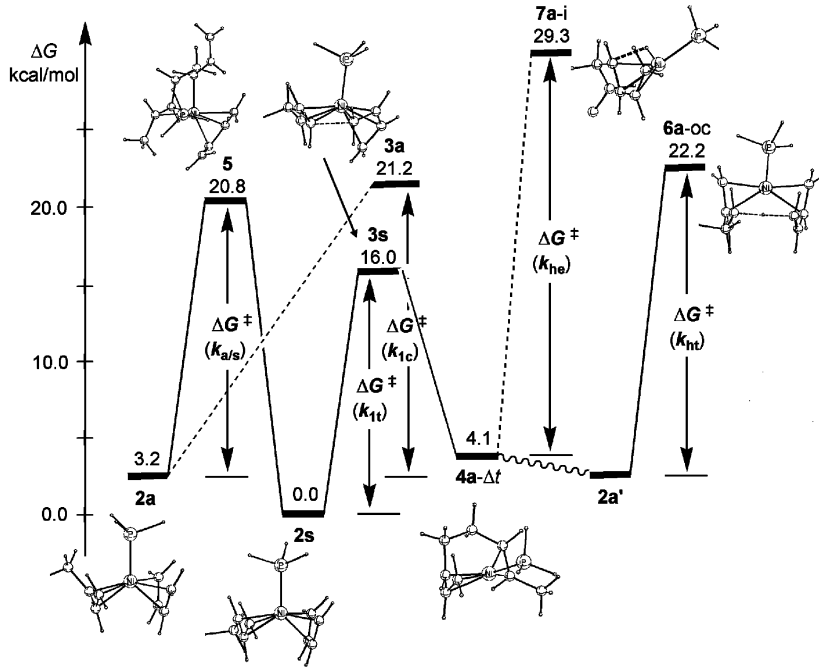

been explored and the respective energetic profiles of which have been predicted. This leads us to suggest the hydrogen atom shift from the C^4(butenyl) carbon of the growing chain to the coordinated monomer as the favorable chain termination mechanism, which preferably takes place outside of the immediate proximity of the nickel atom. The alternative hydrogen elimination mechanism is seen to be kinetically unfeasible as it requires a distinctly higher barrier.

C. Interrelation of Chain Propagation and Chain Termination: Consequences for the Mechanism of Molecular Weight Regulation. Having concluded, from previous sections, that the hydrogen transfer (along k_{ht}) occurring through an outer sphere path is the operative mechanism for chain termination, this section is devoted to the implications for the mechanism of molecular weight regulation. The *cis*-η^4-butadiene π-complex **2** represents the precursor for the principal monomer insertion and allylic *anti*−*syn* isomerization elementary steps of the chain propagation cycle,[32] as well as for the favorable chain termination process of the polymerization course. Accordingly, all these elementary steps obey the same rate law differing only in the magnitude of the unimolecular (with respect to **2**) rate constants r_{1t} (for the preferred *trans*-1,4 generating insertion pathway), $r_{a/s}$, and r_{ht} (via **6a**-oc), respectively (cf. Scheme 3b). For a catalyst to effectively assist the polymerization reaction, chain propagation should be faster than the competitive chain termination ($r_{cp} > r_{ct}$). The length of the generated polymer chain is, to a major extent, determined by the difference in the reaction rate of the dominant respective events, which directly corresponds to the ratio of the associated activation barriers ($\Delta\Delta G^{\ddagger}_{ct-cp}$).

The condensed free-energy profile, consisting of critical elementary processes of the polymerization reaction course, is depicted in Scheme 4;[33,34] the energetics of the chain propagation cycle was taken from our previous investigations.[7e,8] *cis*-Butadiene insertion preferably proceeds through the *trans*-1,4 generating k_{1t} pathway

with an activation energy of 16.0 kcal mol^{-1} ($\Delta G^{\ddagger}(k_t)$, **2s** → **3s**), while the alternative k_{1c} insertion pathway is kinetically impeded due to a barrier of 18.0 kcal mol^{-1} ($\Delta G^{\ddagger}(k_c)$, **2a** → **3a**). For *anti*−*syn* isomerization via $k_{a/s}$ a barrier of 17.6 kcal mol^{-1} ($\Delta G^{\ddagger}(k_{a/s})$, **2a** → **5**) has to be overcome. Accordingly, allylic isomerization requires the highest barrier overall along the chain propagation cycle that preferably generates *trans*-1,4 polymer units, and is therefore rate-controlling for the allylnickel(II) catalyst under consideration. On the other hand, the dominant chain termination process via k_{ht} has an activation barrier of 19.0 kcal mol^{-1} ($\Delta G^{\ddagger}(k_{ht})$, **2a** → **6a**-oc).[33a] As a consequence, chain propagation should be faster than chain termination and the discriminating $\Delta\Delta G^{\ddagger}_{ct-cp}$ ratio is predicted to 1.4 kcal mol^{-1} (k_{ht} vs $k_{a/s}$). This corresponds to a ratio of about 11:1 between insertion and termination events (Maxwell−Boltzmann statistics at 298 K), which indicates that the actual allylnickel(II) catalyst would predominantly produce a *trans*-1,4 polybutadiene of low molecular weight. It should be noted that the real catalytic reaction conditions are treated in an approximate manner by the present investigation (see computational model and method section). The computed $\Delta\Delta G^{\ddagger}_{ct-cp}$ value should therefore be considered as an estimate of the real situation. The delicate energetic balance between chain propagation and chain termination is likely to be influenced by solvent and enhanced catalyst-counterion interactions and furthermore, the electronic and steric properties of the ancillary phosphine ligand L should also be of critical importance in this regard. This will be the subject of forthcoming investigations.

Summary

The present theoretical mechanistic study has, for the first time, examined the chain termination of the transition-metal-catalyzed polymerization of 1,3-dienes for a prototypical allylnickel(II) catalyst. Several conceivable pathways have been scrutinized for the most probable mechanistic alternatives of chain termination; namely (I) the hydrogen elimination mechanism and (II) the hydrogen transfer mechanism. The investigation has been conducted for the well-characterized *trans*-1,4 regulating cationic allylnickel(II) [Ni^{II}(η^3-RC$_3$H$_4$)(*cis*-C$_4$H$_6$)L]$^+$ active catalyst (with L = P(OMe)$_3$ used in computational modeling), employing a gradient-corrected DFT-method.

The hydrogen atom transfer from the C^4(butenyl) carbon of the growing polymer chain to the coordinated monomer (cf. Scheme 2), that occurs from the *cis*-η^4-butadiene π-complex, is suggested as being the operative mechanism for chain termination. This process proceeds preferably in a concerted fashion outside of the immediate proximity of the nickel center. The alternative hydrogen elimination starting from the monomer insertion product, which initially involves hydrogen abstraction from the polymer chain (C^4(butenyl) carbon) to afford an diene hydride complex without participation of a monomer (cf. Scheme 1), requires a distinctly higher kinetic barrier. This makes hydrogen elimination a less likely channel for chain termination.

The *cis*-η^4-butadiene π-complex is the critical species of the entire polymerization reaction course, as it serves as the precursor for the critical monomer insertion and allylic *anti*−*syn* elementary steps of the chain propagation cycle, as well as for the favorable hydrogen transfer chain termination channel. The present study provides, for the first time, a detailed insight into the mechanism of molecular weight regulation for the allylnickel(II)-catalyzed polymerization of 1,3-dienes, for the *trans*-1,4 selective cationic [Ni^{II}(η^3-RC$_3$H$_4$)(*cis*-η^4-C$_4$H$_6$)L]$^+$ (L = PR$_3$, P(OR)$_3$) active catalysts in particular. The influence of the dominant chain propagation and chain termination processes by factors related to medium (solvent, catalyst-counterion interaction) and ligand (electronic and steric properties of the ancillary ligand L) effects needs to be elaborated further in order to obtain a more precise understanding of decisive factors for the controlled generation of a polymer of desired length.

Acknowledgment. The author is grateful to Prof. Dr. Rudolf Taube for his ongoing interest in this research, which serves as a continuous source of stimulation. Excellent service by the computer centers URZ Halle and URZ Magdeburg is gratefully acknowledged.

Supporting Information Available: A table of Cartesian coordinates (in Å) of optimized structures of key species of the investigated chain termination pathways. This material is available free of charge via the Internet at http://pubs.acs.org.

References and Notes

(1) (a) Porri, L.; Natta, G.; Gallazzi, M. C. *Chim. Ind.* **1964**, *46*, 428. (b) Dolgoplosk, B. A.; Babitskii, B. D.; Kormer, V. A.; Lobach, M. I.; Tinyakova, E. T. *Dokl. Akad. Nauk SSSR* **1965**, *164*, 1300. (c) Wilke, G.; Bogdanovic, B.; Hardt, P.; Heimbach, P.; Keim, W.; Kröner, M.; Oberkirch, W.; Tanaka, K.; Steinrucke, E.; Walter, D.; Zimmermann, H. *Angew. Chem., Int. Ed. Engl.* **1966**, *5*, 151. (d) Durand, J. P.; Dawans, F.; Teyssié, Ph. *J. Polym. Sci., Part B:* **1968**, *6*, 757. (e) Porri, L.; Giarrusso, A. In *Comprehensive Polymer Science*; Eastmond, G. C., Ledwith, A., Russo, S., Sigwalt, B., Eds.; Pergamon: Oxford, U.K., 1989; Vol. 4, Part II, pp 53−108. (f) Taube, R.; Schmidt, U.; Gehrke, J.-P.; Böhme, P.; Langlotz, J.; Wache, St. *Makromol. Chem. Macromol. Symp.* **1993**, *66*, 245. (g) Taube, R.; Windisch, H.; Maiwald, St. *Macromol. Symp.* **1995**, *89*, 395.

(2) (a) Teyssié, Ph.; Julemont, M.; Thomassin, J. M.; Walkiers, E.; Warin, R. In *Coordination Polymerization*; Chien, J. C. W., Ed.; Academic Press: New York, 1975; p 327−347. (b) Boor, J., Jr. *Ziegler−Natta Catalysts and Polymerizations*; Academic Press: New York, 1979. (c) Porri, L. In *Structural Order in Polymers*; Ciardelli, F., Giusti, P., Eds.; Pergamon Press: Oxford, U.K., 1981; pp 51−62.

(3) (a) Lazutkin, A. M.; Vashkevich, V. A.; Medvevdev. S. S.; Vasiliev, V. N. *Dokl. Akad. Nauk* **1967**, *175*, 859. (b) Harrod, J. F.; Wallace, L. R. *Macromolecules* **1969**, *2*, 449. (c) Lobach, M. I.; Kormer, V. A.; Tsereteli, I. Yu.; Kondoratenkov, G. P.; Babitskii, B. D.; Klepikova, V. I. *J. Polym. Sci., Polym. Lett.* **1971**, *9*, 71. (d) Druz, N. N.; Zak, A. V.; Lobach, M. I.; Vasiliev, V. A.; Kormer, V. A. *Eur. Polym. J.* **1978**, *14*, 21.

(4) (a) Warin, R.; Teyssié, Ph.; Bourdaudurq, P.; Dawans, F. *J. Polym. Sci., Polym. Lett.* **1973**, *11*, 177. (b) Warin, R.; Julemont, M.; Teyssié, P. Butadiene *J. Organomet. Chem.* **1980**, *185*, 413. (c) Hadjiandeou, P.; Julemont, M.; Teyssié, P. *Macromolecules* **1984**, *17*, 2455.

(5) (a) Taube, R.; Schmidt, U.; Gehrke, J.-P.; Anacker, U. *J. Prakt. Chem.* **1984**, *326*, 1. (b) Taube, R.; Gehrke, J.-P.; Schmidt, U. *J. Organomet. Chem.* **1985**, *292*, 287. (c) Taube, R.; Gehrke, J.-P. *J. Organomet. Chem.* **1987**, *328*, 393. (d) Taube, R.; Gehrke, J.-P.; Radeglia, R. *Organomet. Chem.* **1985**, *291*, 101. (e) Taube, R.; Gehrke, J.-P.; Böhme, P.; Köttnitz, J. *J. Organomet. Chem.* **1990**, *395*, 341.

(6) (a) Taube, R.; Böhme, P.; Gehrke, J.-P. *J. Organomet. Chem.* **1990**, *399*, 327. (b) Taube, R.; Gehrke, J.-P.; Böhme, P.; Scherzer, K. *J. Organomet. Chem.* **1991**, *410*, 403. (c) Taube, R.; Wache, S. *J. Organomet. Chem.* **1992**, *428*, 431. (d) Taube, R.; Langlotz, J. *Macromol. Chem.* **1993**, *194*, 705. (e) Taube, R.; Wache, S.; Sieler, J. *J. Organomet. Chem.* **1993**, *459*, 335.

(7) (a) Tobisch, S.; Bögel, H.; Taube, R. *Organometallics* **1996**, *15*, 3563. (b) Tobisch, S.; Bögel, H.; Taube, R. *Organometallics* **1998**, *17*, 1177. (c) Tobisch, S.; Taube, R. *Organometallics* **1999**, *18*, 5204. (d) Tobisch, S.; Taube, R. *Chem.−Eur. J.* **2001**, *7*, 3681. (e) Tobisch, S. *Chem.−Eur. J.* **2002**, *8*, 4756.

(8) Tobisch, S. *Acc. Chem. Res.* **2002**, *35*, 96.
(9) (a) Harrod, J. F.; Wallace, L. R. *Macromolecules* **1969**, *2*, 449. (b) Harrod, J. F.; Wallace, L. R. *Macromolecules* **1972**, *5*, 685.
(10) Taube, R.; Wache, S.; Kehlen, H. *J. Mol. Catal. A: Chem.* **1995**, *97*, 21.
(11) (a) The formation of a *trans*-1,4-polybutadiene of $M_n \sim 5300$ g mol^{-1} was reported for the following typical reaction conditions:[9] [C_4H_6] = 1.5 M.; [catalyst] = 0.005 M.; conversion = 0.55 M, T = 313 K, in benzene. This corresponds to a ratio of chain propagation and chain termination events of ~98:1. Applying Maxwell−Boltzmann statistics (298 K) to this value gives a $\Delta\Delta G^{\ddagger}$ of ~2.8 kcal mol^{-1} for the respective activation barriers. (b) The formation of a *cis*-1,4-polybutadiene of $M_n \sim 32\,000$ g mol^{-1} was reported for the following typical reaction conditions:[10] [C_4H_6] = 2 M; [catalyst] = 0.0002 M; conversion ~ 0.5 M, T = 298 K, in toluene. This corresponds to a ratio of chain propagation and chain termination events of ~600:1 and a value of $\Delta\Delta G^{\ddagger} \sim 3.8$ kcal mol^{-1} (298 K) for the respective activation barriers. A similar value of M_n was recently reported for a new *cis*-1,4-regulating allylnickel(II) precatalyst.[11c] (c) Campora, J.; del Mar Conejo, M.; Reyes, M. L.; Mereiter, K.; Passaglia, E. *Chem. Commun.* **2003**, 78.
(12) Ashitaka, H.; Inaishi, H.; Ueno, H. *J. Polym. Sci., Polym. Chem. Ed.* **1983**, *21*, 1973.
(13) Taube, R.; Sylvester, G. In *Applied Homogeneous Catalysis with Organometallic Compounds*; Cornils, B., Herrmann, W. A., Eds.; VCH: Weinheim, Germany, 2002, pp 285−315.
(14) Porri, L.; Giarrusso, A.; Ricci, G. *Prog. Polym. Sci.* **1991**, *16*, 405.
(15) (a) The substitution equilibrium between the [$Ni^{II}(\eta^3$-R_3H_4)-L_2]$^+$ precatalyst **1** and the [$Ni^{II}(\eta^3$-RC_3H_4)(*cis*-η^4-C_4H_6)L]$^+$ catalytically active butadiene π-complex **2** is shown in Scheme 3a together with the energetics (ΔG in kcal mol^{-1}). The reported ΔG values differ slightly from that reported in ref 7b, due to the higher basis set level employed in the present study. (b) The energetics for the chain propagation cycle (ΔG, $\Delta G^{\ddagger}$ in kcal mol^{-1}) was taken from our previous theoretical investigations on the [$Ni^{II}(\eta^3$-C_8H_{13})(*cis*-η^4-C_4H_6)P(OMe)$_3$]$^+$ model of the real catalyst (ref 7e, 8). (c) The intrinsic energy required to extend the polybutadienyl chain by an additional C_4 unit in consecutive propagation cycles is excluded from the energetic profile of the chain propagation cycle. (d) The *anti*- and *syn*-butenyl isomers for **2**−**4** and species **6**−**8**, carrying the 1,3-diene-terminated chain of the corresponding cis and trans configuration, are labeled by **a** and **s**, respectively. (e) The depicted transition state structures **6a**, **6s** represent only one of the examined pathways for the hydrogen transfer process (see the text). (f) The depicted transition state structure **7a** represents only one of the examined pathways for the hydrogen elimination process (see the text).
(16) Yasuda, H.; Nakamura, A. *Angew. Chem., Int. Ed. Engl.* **1987**, *16*, 723.
(17) (a) Taube, R.; Gehrke, J.-P.; Böhme, P. *Wiss. Z. Tech. Hochsch. Leuna-Merseburg* **1987**, *39*, 310. (b) Taube, R. In *Metalorganic Catalysts for Synthesis and Polymerization*; Kaminsky, W., Ed.; Springer-Verlag: Berlin and Heidelberg, Germany, 1999; p 531.
(18) (a) Cossee, P. In *Stereochemistry of Macromolecules*; Ketley, A. D., Ed.; Marcel Dekker: New York, 1967; Vol. 1, p 145. (b) Arlman, E. J. *J. Catal.* **1966**, *5*, 178.
(19) Tobisch, S. *Organometallics* **2003**, *22*, 2729.
(20) The competition between *cis*- and *trans*-butadiene for insertion into the η^3-butenyl−Ni^{II} bond was examined in our previous study (ref 7b) for a generic catalyst model with L = PH_3. The reinvestigation for the actual [$Ni^{II}(\eta^3$-C_5H_9)(η^4-C_4H_6)L]$^+$ (L = P(OMe)$_3$) catalyst model revealed that *trans*-butadiene insertion is kinetically disabled by barriers that are 5.6 and 6.0 kcal mol^{-1} ($\Delta\Delta G^{\ddagger}$) higher than that for *cis*-butadiene insertion occurring into the *syn*-η^3 and *anti*-η^3 forms of the butenyl−Ni^{II} bond, respectively.
(21) (a) Faller, J. W.; Thomsen, M. E.; Mattina, M. J. *J. Am. Chem. Soc.* **1971**, *93*, 2642. (b) Lukas, J.; van Leeuwen, P. W. N. M.; Volger, H. C.; Kouwenhoven, A. P. *J. Organomet. Chem.* **1973**, *47*, 153. (c) Vrieze, K. In *Dynamic Nuclear Magnetic Resonance Spectroscopy*; Jackman, L. M., Cotton, F. A., Eds.; Academic Press: New York, 1975.
(22) Tobisch, S.; Taube, R. *Organometallics* **1999**, *18*, 3045.
(23) (a) Ahlrichs, R.; Bär, M.; Häser, M.; Horn, H.; Kölmel, C. *Chem. Phys. Lett.* **1989**, *162*, 165. (b) Treutler, O.; Ahlrichs, R. *J. Chem. Phys.* **1995**, *102*, 346. (c) Eichkorn, K.; Treutler, O.; Öhm, H.; Häser, M.; Ahlrichs, R. *Chem. Phys. Lett.* **1995**, *242*, 652.
(24) (a) Dirac, P. A. M. *Proc. Cambridge Philos. Soc.* **1930**, *26*, 376. (b) Slater, J. C. *Phys. Rev.* **1951**, *81*, 385. (c) Vosko, S. H.; Wilk, L.; Nussiar, M. *Can. J. Phys.* **1980**, *58*, 1200. (d) Becke, A. D. *Phys. Rev.* **1988**, *A38*, 3098. (e) Perdew, J. P. *Phys. Rev.* **1986**, *B33*, 8822.; *Phys. Rev. B* **1986**, *34*, 7406.
(25) (a) Bernardi, F.; Bottoni, A.; Calcinari, M.; Rossi, I.; Robb, M. A. *J. Phys. Chem.* **1997**, *101*, 6310. (b) Jensen, V. R.; Børve, K. *J. Comput. Chem.* **1998**, *19*, 947.
(26) (a) Wachters, A. H. J. *J. Chem. Phys.* **1970**, *52*, 1033. (b) Hay, P. J. *J. Chem. Phys.* **1977**, *66*, 4377. (c) Godbout, N.; Salahub, D. R.; Andzelm, J.; Wimmer, E. *Can. J. Chem.* **1992**, *70*, 560. (d) TURBOMOLE basis set library.
(27) Reed, A. E.; Curtiss, L. A.; Weinhold, F. *Chem. Rev.* **1988**, *88*, 899.
(28) (a) Rossi, A. R.; Hoffmann, R. *Inorg. Chem.* **1975**, *14*, 365. (b) Albright, T. A.; Burdett, J. K.; Whangbo, M.-H. *Orbital Interactions in Chemistry*; John Wiley & Sons: New York, 1985.
(29) (a) *Mechanisms in Inorganic Chemistry*; Basolo, F.; Pearson, R. G., Eds.; G. Thieme Verlag: Stuttgart, Germany, 1973. (b) Cross, R. J. *Chem. Soc. Rev.* **1985**, *14*, 197. (c) Tobe, M. L. In *Comprehensive Coordination Chemistry*; Wilkinson, G., Gillard, R. D., McCleverty, J. A., Eds.; Pergamon Press: New York, 1987; Vol. I, p 81. (d) Cross, R. J. *Adv. Inorg. Chem.* **1989**, *34*, 219. (e) Johnson, L. K.; Killian, C. A.; Brookhart, M. *J. Am. Chem. Soc.* **1995**, *117*, 6414.
(30) Tolman, C. A. *J. Am. Chem. Soc.* **1970**, *92*, 6777.
(31) (a) Such a bis(η^2-diene)-hydride−Ni^{II}L species bears formal resemblance to the well-known trigonal planar bis(η^2-diene)−Ni^0L complexes. (b) Jolly, P. W.; Tkatchenko, I.; Wilke, G. *Angew. Chem., Int. Ed. Engl.* **1971**, *10*, 328. (c) Tobisch, S.; Ziegler, T. *J. Am. Chem. Soc.* **2002**, *124*, 4881.
(32) The chain propagation cycle comprises also of the monomer uptake as a crucial elementary step, which, however, is indicated to occur in a smooth fashion, i.e. without any significant barrier, for allylnickel(II) catalysts.[29] The monomer uptake has explicitly been confirmed in our recent theoretical study as a facile process for the allyltitanium(III)-catalyzed 1,3-butadiene polymerization.[19]
(33) (a) In the investigation of the competition between chain propagation and chain termination the [$Ni^{II}(C_8H_{13})$(*cis*-η^4-C_4H_6)L]$^+$ (L = P(OMe)$_3$) catalyst model was employed for **2**, where the polybutadienyl chain consisted of two C_4-units. This catalyst model allowed a reliable description of elementary processes that are either facilitated (allylic isomerization) or not (monomer insertion, chain termination) by the coordination of the first double bond of the polybutadienyl chain to nickel. (b) The barriers of individual elementary steps are given relative to the corresponding precursor species. (c) The kinetically impeded pathways for chain propagation (via k_{1c}) and chain termination (via k_{he}) are displayed by dashed lines. (d) For the pictorial representation of involved key species, however, L = PH_3 is adopted and the C_8H_{13} polybutadienyl chain is displayed in a shrunken fashion, to simplify the drawing.
(34) Please note, that the energetics for the **1** ⇌ **2** substitution equilibrium (cf. Scheme 3a) has to be taken into account as well in order to make the reported results compatible with experimentally derived kinetic data, since **1s** is prevalent.

MA034369V